JOURNAL DE PHYSIQUE
Colloque C2, supplément au n°3, Tome 44, mars 1983 *page* C2-101

DOPPLER-FREE CONJUGATE EMISSION IN RESONANT GAS MEDIA : LINESHAPE, POLARIZATION PROPERTIES AND SATURATION

D. Bloch, R.K. Raj, K.S. Peng and M. Ducloy

Laboratoire de Physique des Lasers, Université Paris-Nord, 93430 Villetaneuse, France

Résumé - Nous présentons quelques propriétés spécifiques du mélange dégénéré à quatre ondes dans un milieu gazeux résonnant. Nous montrons en particulier que la polarisation de l'onde conjuguée est profondément modifiée par l'effet Doppler résiduel. Pour de fortes intensités d'irradiation, on observe des formes de raies très particulières, dont on montre qu'elles sont typiquement liées à la présence d'une distribution de vitesses atomiques.

Abstract - We analyze some specific features of degenerate four-wave mixing in resonant gas media. One shows that the polarization of the phase conjugate emission is strongly affected by the residual Doppler effect. With saturating intensities, very peculiar emission lineshapes are observed and are shown to be typical effects of the velocity distribution.

Among the various techniques to perform phase-conjugation (PC) of an optical wave, degenerate four-wave mixing (DFWM) in resonant gas media has undergone a remarkable development in the recent years [1]. Let us quote the unique features of this method, which are at the origin of this development : (i) Due to the velocity selection, the PC emission lineshape is Doppler-free [2-4] . This property may be used to build narrow-band optical filters [5]. (ii) Due to the resonant enhancement, the susceptibility of the gas medium saturates for low incident intensities (about 1 mW/mm^2 for an atomic resonance line), which allows one to operate PC mirrors at very low power levels. (iii) The reflectivity strongly depends on the angular separation, θ, between pump and probe beams, and is maximum at grazing incidences ($\theta \to 0$) [3].

In this article, we discuss two kinds of experiments which have been performed in a Neon discharge. In the first one, the polarization properties of phase-conjugate emission are studied and we emphasize the role played by the thermal motion, which tends to vanish the influence of the various atomic relaxation processes on these polarization properties [6]. In the second part, we analyze the origin of the lineshapes observed in the saturated regime, and we show that the inhomogeneous Doppler broadening is fully responsible for the peculiar properties of the PC emission lineshape [7].

I. POLARIZATION PROPERTIES OF PC MIRRORS.

Some of the polarization properties of PC mirrors directly originate in the selection rules imposed by the conservation laws of angular momentum. For instance, the absorption of the angular momentum units carried by the photons absorbed from each pump beam must be compensated by the angular momentum units carried by the photons respectively re-radiated along probe beam and PC beam. The only condition of validity for that law is the assumption that the non-linear medium does not retain angular momentum units (isotropic media). These considerations lead to the predictions of Table I, where the polarizations (π, σ^+, σ^-, $\sigma = \frac{\sigma^+ + \sigma^-}{\sqrt{2}}$) are refered to a fixed quantization axis.

PUMPS	(σ^+,σ^+)			(σ^+,σ^-)			(π,π)		(π,σ)	
PROBE	σ^+	σ^-	π	σ^+	σ^-	π	π	σ	π	σ
PC	σ^+	/	/	σ^-	σ^+	π	π	σ	σ	π

Table I. *Polarization selection rules.*

This table shows that in most cases the polarization of the PC beam is not simply the conjugate of the probe polarization. Nevertheless, the properties of the PC mirror can generally be determined by the knowledge of the emission characteristics for a few sets of polarizations, like the ones depicted in Table I. The essential requirement is that the PC field depends linearly on each of the three incident fields [i.e. the nonlinearity must be a third-order nonlinearity]. This implies very low incident intensities in the case of resonant gas media.

In the following, we will restrict ourselves to the case when all the incident beams are linearly polarized. This in general implies that the PC beam is also linearly polarized . With the assumption of weak non-saturating incident intensities, only two types of configuration have to be studied : (i) Pumps co-polarized, (ii) pumps orthogonally polarized. The quantization axis is chosen along the polarization of the forward pump beam $\vec{e}_f = \vec{u}_z$ (π polarization) and the angles α_o and α_r define the polarization of the probe beam and of the PC beam respectively :

$$\vec{e}_o = \cos \alpha_o \, \vec{u}_z + \sin \alpha_o \, \vec{u}_x \qquad (1)$$

$$\vec{e}_r = \cos \alpha_r \, \vec{u}_z + \sin \alpha_r \, \vec{u}_x \qquad (2)$$

From Table I, one easily gets the following polarization laws :

(i) For parallel pump polarizations : $\operatorname{tg} \alpha_r = \operatorname{Ctg} \alpha_o$ (3)
with $C = g(\sigma)/g(\pi)$, where $g(\sigma)$ and $g(\pi)$ are respectively the (amplitude) efficiency of a σ or a π polarized probe.

(ii) For orthogonal pump polarizations : $\operatorname{tg} \alpha_o \operatorname{tg} \alpha_r = D$ (4)
with $D = f(\pi)/f(\sigma)$, where $f(\sigma)$ and $f(\pi)$ are respectively the (amplitude) efficiency of a σ or a π polarized probe.

These rules have been experimentally verified on various Ne transitions in a discharge. A schematic of the set-up is given in Fig.1. Incident intensities are typically kept below 0.5 mW/mm^2 to avoid saturation effects. The polarization of the PC beam (determined by rotating the analyzer to the extinction) is independent of the frequency detuning in the case of non-saturating intensities. Although the PC reflectivity was quite low [typically $10^{-4} - 10^{-6}$ with low pump intensities ; up to 10^{-3} with saturation] the accuracy of the measurement in most cases is as good as 1° (including the slight and unavoidable depolarization induced by the beam splitters).

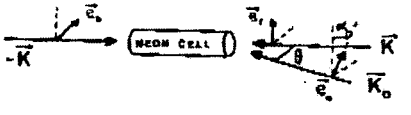

Fig.1 *Experimental scheme*

To determine the constants C and D requires to go deeper in the physical processes of the PC emission. One knows that in gases, the interaction ordering consists in an ab-

sorption of one photon of the forward pump (f) beam, followed by the emission of one photon of the probe beam, so that a (large-spacing) grating is created ; the backward pump beam (b) is thus diffracted by this grating. Other processes, like the creation of a small-spacing grating by the pump (b) and probe are not considered here since they are destroyed very quickly by the atomic thermal motion [3-4]. If the pump beam (f) and the probe have identical polarizations, a spatial modulation of the intensity of the resulting field appears, producing a population grating in the medium. On the other hand, when the pump (f) and the probe have orthogonal polarizations, the intensity is no longer spatially modulated, so that in the framework of a scalar theory [e.g. for a non-degenerate two-level system] the PC emission should be forbidden. Actually, the spatial variation of the polarization induces spatially-modulated coherent effects and there is a PC field produced by the diffraction of the backward pump on a grating of Zeeman coherence induced between magnetic sublevels.

In order to get a general expression of C and D, we give the explicit value of the PC field amplitude, $\vec{\mathcal{E}}_r$, resulting from a third-order calculation in the tensorial formalism [8], in the limit of large Doppler broadenings, and with $\theta \ll 1$ [9].

For parallel pump polarizations ($\vec{e}_f = \vec{e}_b = \vec{u}_z$)

$$\vec{\mathcal{E}}_r = \mathcal{E}(\nu)\ [h \cos \alpha_o\ \vec{u}_z + f \sin \alpha_o\ \vec{u}_x] \tag{5}$$

For orthogonal pump polarizations ($\vec{e}_f = \vec{u}_z, \vec{e}_b = \vec{u}_x$)

$$\vec{\mathcal{E}}_r = \mathcal{E}(\nu)\ [g \sin \alpha_o\ \vec{u}_z + c \cos \alpha_o\ \vec{u}_x] \tag{6}$$

In these expressions, $\mathcal{E}(\nu)$ represents the frequency dependence of the emission amplitude :

$$\mathcal{E}(\nu) = \frac{\pi}{(Ku)^2\,\theta}\ \frac{\mathcal{C}}{\Gamma_{eg} - i\nu} \tag{7}$$

where ν is the frequency detuning relatively to the transition $(g,J_g) \rightarrow (e,J_e)$, $\nu = \omega - \omega_{eg}$; Ku is the Doppler width, Γ_{eg} the optical linewidth and $\mathcal{C}$ a constant, independent of the polarizations, and proportional to the amplitude of each incident field

$$\text{and} \quad c = \sum_{k=0,2} (-)^{k/2}\, \zeta_k \qquad d = \sum_{k=1,2} \frac{3}{2}\, \zeta_k$$
$$f = \sum_{k=1,2} (-)^{k}\, \frac{3}{2}\, \zeta_k \qquad h = \sum_{k=0,2} \left(1+\frac{k}{2}\right) \zeta_k \tag{8}$$

$$\text{with } \zeta_k = \begin{Bmatrix} 1 & 1 & k \\ J_e & J_e & J_g \end{Bmatrix}^2 \psi^{\,k}_{e} + \begin{Bmatrix} 1 & 1 & k \\ J_g & J_g & J_e \end{Bmatrix}^2 \psi^{\,k}_{g} \tag{9}$$

$$\psi^{\,k}_{\beta} = \psi\left(\frac{\Gamma_\beta(k)}{Ku\theta}\right) \qquad [\beta = e,g] \tag{10}$$

$\psi(x)$ is the function

$$\psi(x) = e^{x^2}\left[1 - \frac{2}{\sqrt{\pi}} \int_o^x e^{-t^2}\, dt\right] \tag{11}$$

$\Gamma_\beta(k)$ is the relaxation rate for the tensorial observable of rank k [$\Gamma_\beta(k)$ is respectively associated with the relaxation of the population (k = 0), of the atomic orientation (k = 1) and of the alignment (k = 2) of level β]. These formulae are establi-

shed in the case of a small residual Doppler broadening, [$\Gamma_{cg} >> Ku\theta$, $\Gamma_g(k)$] and, for the sake of simplicity, cascade effects induced by spontaneous emission are neglected (if not, slight changes should be brought to ζ_k). The expression of C and D (Eq. 3 and 4) is then obvious :

$$C = f/h \quad ; \quad D = c/d \qquad (12)\ (13)$$

These expressions of C and D show that the efficiency for a definite set of polarizations depends mainly on :

(i) the relaxation processes in the gas medium, which determine the intrinsic lifetime of the gratings : a pressure dependence is expected due to collisional broadening. In general, the relaxation mechanisms are not scalar, which implies that population gratings and Zeeman coherence gratings are not governed by the same relaxation constants ($k = 0,2$ for the population ; $k = 1,2$ for the Zeeman coherences).

(ii) the residual Doppler broadening, $Ku\theta$: the gratings are washed out in a mean time $(Ku\theta)^{-1}$ (Ku : Doppler width). This decay, induced by the thermal motion, tends to overcome the effects of the various intrinsic relaxation processes.

(iii) the geometrical coefficients which are related to the angular momentum of the atomic levels involved in the transition.

Let us consider experiments performed on the $1s_5(J = 2) \rightarrow 2p_9(J = 3)$ transition of Neon. All the parameters of the relaxation are known (see Table II). The residual Doppler-broadening is $Ku\theta = 37$ MHz ($\theta = 30$ mrads). In Fig.2, are drawn three theoretical curves for parallel polarizations : $C = 1.8$ and $C = -0.05$ are the theoretical predictions when the Doppler shortening is neglected [$\theta = 0$ in Eqs. (5-12)] for two different experimental conditions, respectively 0.6 Torr of a mixture He(95%) + Ne(5%) and 0.5 Torr of pure Ne. $C = -0.41$ is the theoretical prediction [10] for $\theta = 30$ mrads (independently of the discharge pressure) and is in very good agreement with the experimental data (Fig.2). This demonstrates the crucial role played by the Doppler shortening of the grating lifetime, which completely overcomes the drastic effect of collisions predicted at $\theta = 0$. The residual Doppler effect, even in the absence of lineshape broadening (since $Ku\theta < \Gamma_{cg}$), is able to alter the polarization properties of PC mirrors in a very strong manner. It shows also that, to detect specific effects of collisions in FWM (like break of a selection rule by depolarizing collisions), the collinear configuration ($\theta = 0$) is often the only appropriate one.

k	$1s_5$	$2p_9$
0	~15 kHz	8.2 MHz
1	0.7 MHz/T	8.2 MHz + 4.4 MHz/T
2	1 MHz/T	8.2 MHz + 4.4 MHz/T

Table II. *Variations of $\Gamma(k)$ with Ne pressure* [11] ($1s_5$ *is a metastable level*).

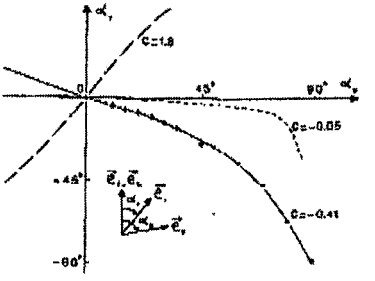

Fig.2 *Rotation of the PC signal polarization for parallel pump polarizations. Transition* $1sq(J = 2) \rightarrow 2pq(J = 3)$ $\lambda = 640$ *nm. (o): 0.6 T of Ne (5%) - He(95%) ;(+):0.5 T of pure Ne. The plotted curves follow* $tg\ \alpha_r = Ctg\ \alpha_o$, *with* $C = 1.8, -0.05, -0.41$, *as indicated (see text).*

Similar conclusions can be derived from the analogous experiment with cross-polarized pumps (Fig.3). In this case, it must be noticed that D is almost equal to 1 ($n = 1.11$) which means that the efficiency of the PC mirror is nearly independent of the probe polarization. In the hypothesis of a single relaxation time model, or if the Doppler effect is strongly predominant, one finds exactly $D = 1$. This follows from Eqs.(8-12)

for $Ku\theta \gg \Gamma_\beta(k)$ (so that $\psi^k_\beta = 1$ which implies c = d from symmetry rules). In this model, the PC mirror behaves like a half-wave birefringent mirror with the neutral axes along the bisectors of the pump polarizations. Experimentally, D = 1.11 leads to an angular deviation from this description which never exceeds 3°.

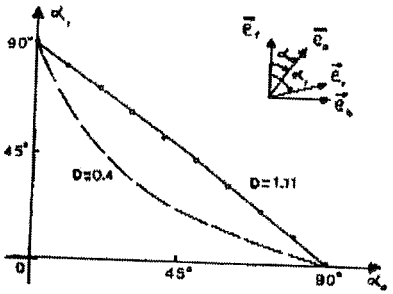

Fig.3 *Polarization rotation for cross-polarized pumps* [λ=640nm, p=0.6T, Ne 5% He 95%] . *The plotted curves follow :* $tg\ \alpha_o\ tg\ \alpha_r = D$, with D = 1.11 or 0.4

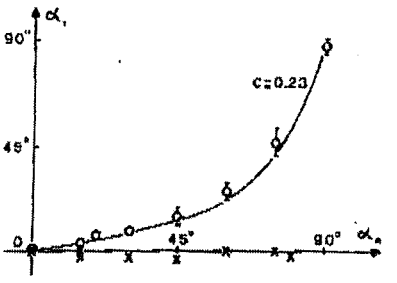

Fig.4 *Polarization rotation for parallel-pump polarizations.* (x)λ=607nm, $1s_4(J=1) \rightarrow 2p_3(J=0)$. *Due to selection rules, the PC polarization is identical to the pump polarization.* (o)λ=614nm, $1s_5(J=2) \rightarrow 2p_6(J=2)$. *The solid curve follows :*

$tg\ \alpha_r = 4\ tg\ \alpha_o/17 = 0.23\ tg\ \alpha_o$

On the opposite, when the pumps are co-polarized, the PC mirror is dichroic [reflectivity depending upon the probe polarization], even in a single relaxation model. An extreme example is given in the case of a J = 1 → J = 0 transition, for which there is no reemission if the probe is σ polarized (Fig.4). This selection rule can be deduced from Eqs. (8,9,12) or understood from Fig.5 [18]. We give below the J dependence of the constant C calculated in a single relaxation constant model [$\psi^k_\beta = 1$ in Eqs. (8 - 12)].

$$\text{for a } J \rightarrow J+1 \text{ transition, } C = -J(2J+4)/(4J^2+8J+5) \qquad (14)$$

$$\text{for a } J \rightarrow J \text{ transition, } C = (J-1)(J+2)/(3J^2+3J-1) \qquad (15)$$

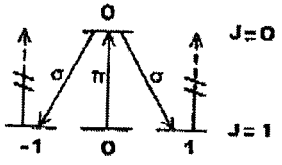

Fig.5 *Selection rule for a J = 1 → J = 0 transition in the case of π polarized pumps and σ polarized probe.*

Hence, a probe with the same polarization π as the two pumps is more efficiently reflected than a σ polarized probe. This result is due to the anisotropy of the PC mirror induced by the two pumps beams which define a preferential polarization axis. The quantitative difference between π and σ probe reflectivities can be considerable : of the order of 20 for a J=2 → J=2 transition [λ = 614 nm, $1s_5 \rightarrow 2p_6$] as it was seen experimentally (Fig.4) (C = 4/17 and the ratio of PC intensities is given by $|C|^2$). Due to the existence of a preferential axis, the PC mirror with parallel pump polarizations is a non reciprocal mirror : after two PC reflexions, the final polarization does not come back to the initial one. This last property could be of great interest to build unidirectional ring PC resonator [6].

In the particular case of the $1s_5 \rightarrow 2p_6$ transition, the PC efficiency is always very small, due to the optical pumping of the $1s_5$ metastable state [the $2p_6$ level can de-

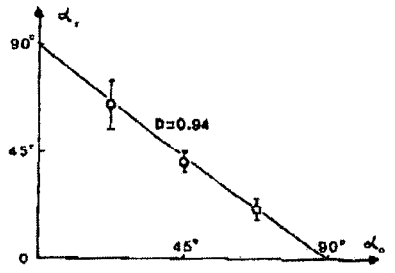

Fig.6 *Polarization rotation for cross-polarized pumps* [λ = 614 nm, p = 0.6 T, Ne 5%, He 95%].

cay to $1s_2$ and $1s_4$]. The extinction ratio of the analyzer is thus rather bad. This explains the relatively large error bars in the measurements performed for a probe polarization nearly orthogonal to the pump polarization [in that case, the efficiency is decreased by another order of magnitude — see Fig.4, for $\alpha_o = 75°$]. The same remark applies to the configuration with orthogonally polarized pump beams. The theoretical value D = 0.94 (in good agreement with the experiments — see Fig.6) demonstrates that the description by a single relaxation rate is once again quite satisfactory. Hence, the ratio $R_m^{//}/R_m^{\perp}$ between the maximum reflectivities for the two types of mirrors [respectively with pumps co-polarized and pumps orthogonally polarized] is given by $|h/c|^2 = |h/d|^2$.

Numerically, one gets :

$$\text{for a } J \to J+1 \text{ transition, } R_m^{//}/R_m^{\perp} = [(8J^2 + 16J + 10)/(6J^2 + 12J + 7)]^2 \qquad (16)$$

$$\text{for a } J \to J \text{ transition, } R_m^{//}/R_m^{\perp} = [(6J^2 + 6J - 2)/(2J^2 + 2J + 1)]^2 \qquad (17)$$

In the case of a J = 2 → J = 2 transition, this ratio is nearly equal to 7. All these numerical results emphasize the importance of polarization studies in the determination of PC efficiencies.

These studies show that there is no hope to build a "vectorial phase-conjugate" mirror [12] [for which the PC polarization is the conjugate of the probe polarization] with linearly polarized pumps : indeed, a birefringent behaviour (for cross-polarized pumps), or a linear dichroism (for parallel-polarized pumps) are obviously contradictory with vectorial phase-conjugation. Actually, vectorial phase-conjugation at grazing incidence necessarily requires that the two pumps have circular counterrotating polarizations (e.g. pump f is σ^+, pump b is σ^-) [13]. A necessary condition is that there is no circular dichroism, so that any linear polarization 0 is reflected identically to itself. This condition becomes sufficient if θ is small enough, so that the probe polarization does not own any π component. We give below the expression of the PC field amplitude, equivalent to Eq.(6), for the following configuration :

$$\vec{e}_f = \vec{u}_+ \ , \ \vec{e}_b = \vec{u}_- \ , \ \vec{e}_o = \frac{1}{\sqrt{2}} \left[e^{i\varepsilon_o} \vec{u}_- + e^{-i\varepsilon_o} \vec{u}_+ \right] \qquad (18)$$

where $\vec{u}_+$ and $\vec{u}_-$ are respectively the unit vectors defining σ^+ and σ^- polarizations and ε_o the angle $(\vec{e}_o, \vec{u}_x)$:

$$\vec{\mathcal{E}}_r = \frac{1}{\sqrt{2}} \mathcal{E}(\nu) \left[\ell_- e^{-i\varepsilon_o} \vec{u}_+ + \ell_+ e^{i\varepsilon_o} \vec{u}_- \right] \qquad (19)$$

$$\text{with } \ell_- = \sum_{k=0,1,2} 3(2k+1) \begin{pmatrix} 1 & 1 & k \\ 1 & 1 & -2 \end{pmatrix}^2 \zeta_k = 3\,\zeta_2$$

$$\ell_+ = \sum_{k=0,1,2} (-)^k 3(2k+1) \begin{pmatrix} 1 & 1 & k \\ 1 & -1 & 0 \end{pmatrix}^2 \zeta_k = \zeta_o - 3\,\zeta_1/2 + \zeta_2/2 \qquad (20)$$

In general, ℓ_- and ℓ_+ are not equal, due to the fact that ℓ_- depends only on tensorial observables of rank 2. A simple explanation of this fact is given in Fig.7 : for a σ^- probe, the PC emission is due to the creation of a Zeeman coherence between sub-

levels m and m+2 while the population grating (for a σ^+ probe) depends on the parameters of population, orientation and alignment. However, some interesting results can be deduced from the following sum rule :

$$3\begin{Bmatrix} 1 & 1 & 2 \\ J_\beta & J_\beta & J_\alpha \end{Bmatrix}^2 = \begin{Bmatrix} 1 & 1 & 0 \\ J_\alpha & J_\alpha & J_\beta \end{Bmatrix}^2 - \frac{3}{2}\begin{Bmatrix} 1 & 1 & 1 \\ J_\alpha & J_\alpha & J_\beta \end{Bmatrix}^2 + \frac{1}{2}\begin{Bmatrix} 1 & 1 & 2 \\ J_\alpha & J_\alpha & J_\beta \end{Bmatrix}^2 \qquad (21)$$

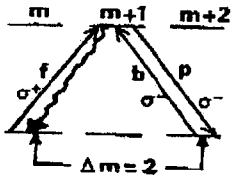

Fig.7 *Scheme of the interaction when pumps are σ^+,σ^- and probe is σ^-. The grating induced by pump f and probe is a $\Delta m = 2$ Zeeman coherence grating.*

(i) The relaxation of each level is described by a single rate [$\Gamma_\beta(k) = \gamma_\beta$, i.e. $\psi^k_\beta = \psi_\beta$] : ℓ_+ and ℓ_- are equal if J_e and J_g can be interchanged in the expression of ζ_k [Eq.9]. Hence, vectorial phase-conjugation is achieved if the incident fields interact with a $J \to J$ transition, but not for a $J \to J+1$ transition (since $\begin{Bmatrix} 1 & 1 & k \\ J_\alpha & J_\alpha & J_\beta \end{Bmatrix}^2 \neq \begin{Bmatrix} 1 & 1 & k \\ J_\beta & J_\beta & J_\alpha \end{Bmatrix}^2$, if $J_\beta \neq J_\alpha$).

(ii) In a single relaxation constant model $\psi^k_\beta = \psi_c - \psi_g$, one finds $\ell_+ = \ell_-$.

Then, in most experiments, when the residual Doppler effect is predominant, a nearly perfect vectorial phase-conjugator is created with σ^+/σ^- pumps, independently of the transition considered. It can be noticed also that vectorial phase-conjugation is no longer possible when the angular separation θ increases : the requirement of an equal efficiency for both π and σ probes is generally not satisfied, as seen easily in the case of a $J = 0 \to J = 1$ transition : a selection rule forbids the reemission when the probe is π polarized.

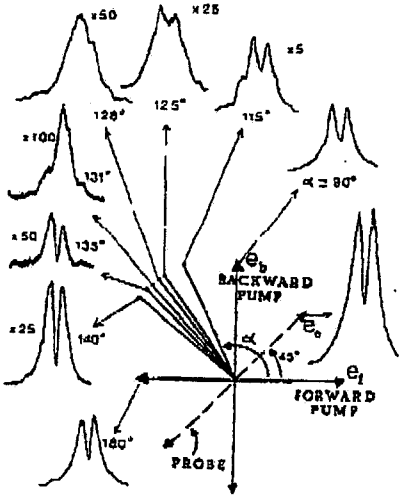

Finally, a much more intricate situation is observed when the incident beams saturate the medium. The emission lineshape is no longer a Lorentzian (Fig.8), but the most striking feature is that the saturated lineshape depends on the analyzed polarization. This observation reflects a complicated theoretical situation. However, it is worth noticing that such a type of experiment could be used to study high-order nonlinearities, for example if the analyzer is set to prevent the transmission of the third-order component.

Fig.8 *Lineshape of the saturated PC emission versus analyzer angle, α, for cross-polarized pumps, and probe at $\alpha_o = 45°$ [λ = 640 nm, p = 0.15 T]. Note the lineshape change around near-extinction of the PC field [α = 131°].*

II. SATURATION BEHAVIOUR IN RESONANT DFWM.

Structures induced by saturation effects in the emission lineshape (Fig.9a) have been observed from the first experiments in gas media [2], but not fully understood. Two interpretations for the lineshape splitting have been currently suggested (i)

one is based upon the a.c. Stark splitting produced by a strong resonant irradiation (ii) the second one assumes that, in the nonlinear susceptibility χ_{NL}, the imaginary component (absorption-like lineshape) saturates much faster than the real component (dispersion-like lineshape), so that the intensity lineshape (proportional to $|\chi_{NL}|^2$) is essentially the square of a dispersion curve, exhibiting a dip on line center. Until now, the validity of these interpretations could not be tested, since the experimental information was limited to the knowledge of the intensity lineshapes. It appeared however that the idea of an a.c. Stark splitting had to be rejected : for transitions between degenerate levels, substructures should be expected, due to the various Rabi frequencies and Stark splittings associated with transitions between different magnetic sublevels. Up to now, such substructures have not been observed (see Fig.9a).

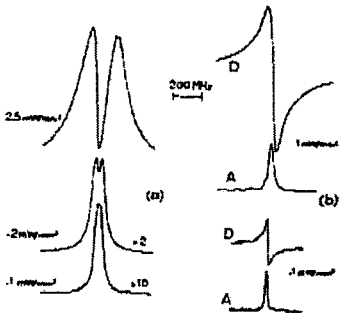

Fig.9 *PC emission lineshape for various powers of the standing pump wave* [Ne discharge, λ = 640 nm, $1s_5$ (J=2) + $2p_9$ (J=3)]. *The probe intensity is non-saturating* [< 0.1 mW/mm^2]. (a) *Frequency dependence of the intensity lineshape.* (b) *Heterodyne detection of the PC field, amplitude* [26 = 44 MHz]. A: *absorption,* D: *dispersion.*

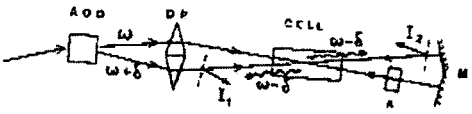

Fig.10 *Basic scheme for heterodyne detection* [A : *attenuator used in the experiments of* Fig.11].

In order to get direct information on the complex nonlinear susceptibility, we have analyzed the PC emission by using optical heterodyne detection techniques. The optical set-up (Fig.10) consists of two standing-waves issuing from an acousto-optic deflector (AOD), operated with two RF frequencies, so that a fixed frequency shift is created between the pump wave (frequency ω) and the probe wave at frequency $\omega + \delta$. These two beams cross inside a Ne discharge cell, thanks to a double prism DP, and are retro-reflected by a double plane mirror. This set-up enables us to work with collimated beams, so that the saturation is constant over the whole interaction region. By an adequate RF input in the AOD, the probe intensity is always kept at non-saturating level. Due to nearly degenerate FWM processes, two PC fields at $\omega - \delta$ are reemitted along the probe direction and detected through their heterodyne beating at frequency 2δ with either probe [detection along I_1 or I_2 (see Fig.10)]. The beat intensity is proportional to the amplitude of the PC field, and using a high-frequency phase-sensitive (lock-in) detection, signals proportional to the real or imaginary parts of χ_{NL} can be obtained.

Such absorption and dispersion components are shown in Fig.9b. At low intensity, as predicted in a third-order theory [see Eq.7], the lineshapes are Doppler-free Lorentzians satisfying to a Kramers-Kronig-type relationship (absorption and dispersion have the same amplitude). For saturating pump intensities, the Kramers-Kronig relation breaks down, and the amplitude of the dispersion becomes considerably larger than the one of the absorption component. This provides a direct experimental evidence for the dispersive origin of the lineshape splitting. Such a saturation behaviour has been previously inferred by Woerdman and Schuurmans [14] from a simplified model based on the nonlinear response of stationary two-level atoms to a resonant irradiation. The validity of such a model is questionable since one knows, from a rigorous calculation performed by Abrams and Lind [15] that, in the absence of inhomogeneous broadening, the saturation induced by an intense standing pump wave cannot produce any lineshape splitting (at least when propagation effects are neglected). This shows that the inhomogeneous broadening coming from the velocity distribution

has a decisive influence on the saturated emission lineshape - in spite of the fact that the latter is Doppler-free -.

We have seen above that the thermal motion unbalances the effect of either f or b pump wave by altering the grating decay in a different way. Another important consequence of the atomic motion has been observed on the saturated lineshape. To discriminate between the optical saturation induced by either pump wave, we have performed a series of experiments in which the return pump wave was strongly attenuated in order to isolate the saturation produced by a single, intense running pump wave. Due to the symmetry of the set-up, the effects of a forward-pump-induced saturation and of the equivalent backward saturation are easily compared by moving the photodetector from I_1 to I_2 (Fig.10). At this point, it is important to recall that, in a "stationary-atom" theory, pumps f and b play a symmetrical role, i.e. I_1 and I_2 should yield the same signal. As shown below, this is not at all the case.

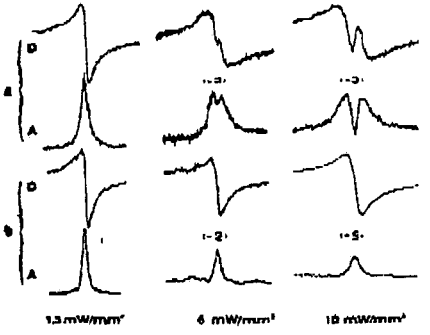

Fig.11 PC emission lineshape at λ = 607 nm ($J=1 \rightarrow J=0$ transition) with a single saturating pump. (a) Forward saturation (I_1, see Fig.10). (b) Backward saturation (I_2, see Fig.10).

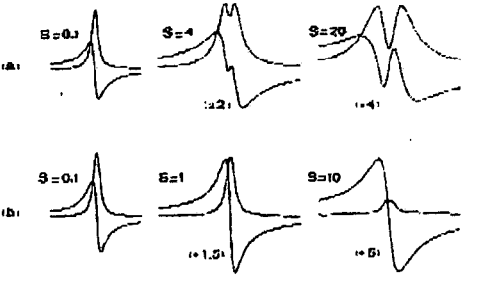

Fig.12 Theoretical emission lineshape in a single lifetime model, for different values of the normalized pump intensity, S. (a) Forward saturation, (b) Backward saturation.

The experiments have been performed on the $1s_4(J=1) \rightarrow 2p_3(J=0)$ (λ = 607 nm) transition of Ne, with crossed (linear) polarizations between the incident beams (issuing from the AOD) and the return beams. Experimental lineshapes are shown in Fig.11. In the case of forward saturation (Fig.11a), absorption and dispersion have nearly the same amplitude, independently of the saturating intensity, but their lineshapes own very peculiar structures at line center. These structures reach full-scale amplitude for strong saturation. Another essential point is the fact that the overall amplitude of the signal, after reaching a maximum, decreases to zero, when the intensity of the pump f alone is increased. In the case of backward saturation (Fig.11b), the behaviour resembles the one observed for standing pump wave saturation : the dispersive component of the susceptibility is predominant, no structure appears in the lineshapes, and an increase of the pump b intensity alone leads to a non-zero asymptotic value for the signal amplitude, so that the signal can be at least one order of magnitude larger than with an equivalent forward saturation. All these features have been interpreted with an adequate density-matrix treatment [16]. The main assumptions are the following ones :

(i) The theoretical calculation is limited to first perturbation order in the probe and weak pump fields, but takes into account arbitrary intensities of the saturating pump beam via a nonperturbative treatment.

(ii) The $J=1 \rightarrow J=0$ transition interacting with the cross-polarized fields is described as a three-level system (with degenerate frequencies) in which pump f and probe interact with one transition, while pump b interacts with the coupled transition. Note that this approach eliminates the problems related to spatial hole-burning.

(iii) Probe and pump cross at grazing incidence ($\theta = 0$). This approximation is valid when the residual Doppler broadening, ($Ku\theta$=12MHz), is small compared with the linewidth, Γ. We also neglect the frequency shift (δ = 22 MHz) between pump and probe in comparison with Γ, and take all the incident frequencies to be equal.

(iv) Propagation effects are not considered. The gas medium is assumed to be optically thin (linear absorption of the order of 5% in the interaction region).

With these hypotheses, in the Doppler limit approximation ($Ku \gg \Gamma$) the velocity integration of the final expression may be performed analytically.

Theoretical curves are shown in Fig.12 (for a single relaxation time model). They reproduce the main experimental observations [existence of structures, dispersive nature of the nonlinearity, asymptotic behaviour, ...]. The same calculation also yields intensity lineshapes. As shown in Fig.13, even with a single saturating pump, the saturated lineshape exhibits a double peak structure. The dip at line-center in the case of forward saturation is not of dispersive origin — as in the case of backward saturation —, but is due to the structures of the absorption component itself. The splitting is proportional to the Rabi frequency Ω, and equal to $3\Omega/2$ in a single relaxation constant model. The difference between peak reflectivity for forward and backward saturation is shown in Fig.14. For relatively moderate forward saturation, the reflectivity drops down to zero. It should be noted that the splitting in the intensity lineshape appears faster for backward saturation than for forward saturation. This anisotropic behaviour, predicted by our theoretical model which takes into account the atomic motion, has been observed by Roulnois et al. [17] in slightly different conditions. (In their experiment, both pump beams are saturating, but with very different intensities).

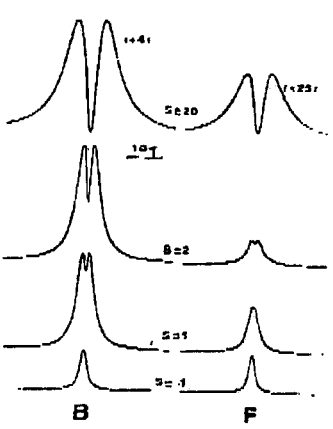

Fig.13 *Theoretical intensity lineshapes in a single lifetime model for different values of the normalized pump intensity.* (B) *backward saturation,* (F) *forward saturation.*

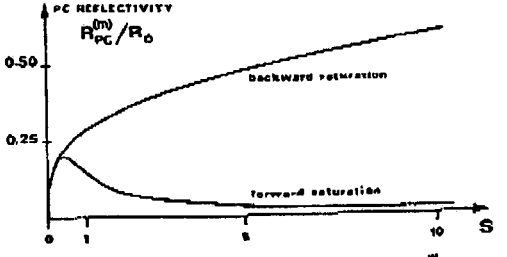

Fig.14 *Theoretical peak reflectivity* R_{PC}^{m} *vs* (f or b) *saturating pump intensity.* R_0 *is the asymptotic value of the reflectivity in the case of backward saturation. The peak reflectivity* R_{PC}^{m} *is defined as the maximum value in the curves of Fig.13.*

In conclusion, this work demonstrates the crucial importance of the atomic motion for the understanding of FWM in gas media. We have shown that the polarization properties of PC mirrors are deeply altered by the thermal motion, and exhibit quasi-general characteristics only based on the angular momentum values, independently of the considered gas media. This allows a perfect control of the PC polarization by an adequate choice of the input (pump and probe) polarizations. As regards the emission lineshape, the directional anisotropy of the saturation effects, or the dispersive origin of the intensity lineshape in the case of an intense standing pump wave, which have been experimentally demonstrated by means of heterodyne detection techniques, are phenomena also produced specifically by the thermal motion (unpredictible for stationary atoms). A theoretical analysis of the saturation induced by an intense standing pump wave is in progress. It can already be suggested that, in gas media, an op-

timum intensity ratio between pump f and pump b should exist. Future theoretical development should also include the effect of high-order nonlinearities on the PC polarization.

This work was supported in part by "Direction des Recherches, Etudes et Techniques" (Paris). The "Laboratoire de Physique des Lasers" is a laboratory associated with the "Centre National de la Recherche Scientifique" (C.N.R.S.).

REFERENCES.

[1] M. DUCLOY in Festkörperprobleme - Advances in Solid State Physics (Vieweg, Braunschweig, 1982), Vol XXII, pp 35-60, and references therein.

[2] P.F. LIAO, D.M. BLOOM and N.P. ECONOMOU, Appl. Phys. Lett. 32, 813 (1978).

[3] M. DUCLOY and D. BLOCH, J. Phys. (Paris) 42, 711 (1981).

[4] S.M. WANDZURA, Opt. Lett. 4, 208 (1979).

[5] J. NILSEN, N.S. GLUCK and A. YARIV, Opt. Lett. 6, 380 (1981).

[6] M. DUCLOY, R.K. RAJ and D. BLOCH, Opt. Lett. 7, 60 (1982) ; D. BLOCH and M. DUCLOY, J. Phys. B, 14, L471 (1981).

[7] D. BLOCH, R.K. RAJ, K.S. PENG and M. DUCLOY, Phys. Rev. Lett. 49, 719 (1982).

[8] A. OMONT in Progress in Quantum Electronics (Oxford-Pergamon) (1977) Vol 5, pp 69-138 ; B. DECOMPS, M. DUMONT and M. DUCLOY in Laser Spectroscopy of Atoms and Molecules (Topics in Applied Physics, Vol 2 - Springer Verlag, 1976) pp 283-347.

[9] M. DUCLOY and D. BLOCH, to be published.

[10] All these theoretical values are calculated with spontaneous cascade effects taken into account.

[11] M. PINARD and M. LEDUC, J. Phys. (Paris) 38, 609 (1977) ; C.G. CARRINGTON and A. CORNEY, J. Phys. B 4, 849 (1971).

[12] See also the work of S. SAIKAN in these proceedings.

[13] B.Ya. ZEL'DOVICH and V.V. SKUNOV, Sov. J. Quantum Electron. 9, 379 (1979).

[14] J.P. WOERDMAN and M.F.H. SCHUURMANS, Opt. Lett. 6, 239 (1981).

[15] R.L. ABRAMS and R.C. LIND, Opt. Lett. 2, 94 (1978) and 3, 205 (1978).

[16] D. BLOCH and M. DUCLOY, to be published.

[17] J.L. BOULNOIS et al. in these proceedings.

[18] Similar selection rules have been observed in Na by Lam et al. [Appl. Phys. Lett. 38, 977 (1981)].